

# Specific and Rapid Scintigraphic Detection of Infection with $^{99m}\text{Tc}$ -Labeled Interleukin-8

Huub J.J.M. Rennen, Otto C. Boerman, Wim J.G. Oyen, Jos W.M. van der Meer, and Frans H.M. Corstens

*Departments of Nuclear Medicine and Internal Medicine, University Medical Center Nijmegen, Nijmegen, The Netherlands*

Interleukin-8 (IL-8) is a chemotactic cytokine involved in activation and recruitment of neutrophils to areas of infection. In our previous studies in rabbits we tested  $^{123}\text{I}$ -labeled IL-8 for its potential to image infections and showed that IL-8 rapidly and efficiently accumulated in infectious foci. However, labeling of IL-8 with  $^{123}\text{I}$  is costly and laborious and the specific activity of the preparation was low. In this study IL-8 was labeled with  $^{99m}\text{Tc}$  through the hydrazinonicotinamide (HYNIC) chelator. **Methods:** The leukocyte receptor-binding capacity of the preparation was determined in vitro. Rabbits with *Escherichia coli* abscesses were injected intravenously with 7 MBq  $^{99m}\text{Tc}$ -HYNIC-IL-8. Biodistribution of the radiolabel was determined by gamma camera imaging and tissue counting at 8 h after injection.  $^{99m}\text{Tc}$ -HYNIC-lysozyme was used as a size-matched control. **Results:** The leukocyte receptor-binding capacity of the  $^{99m}\text{Tc}$ -HYNIC-IL-8 preparation was preserved as determined in vitro, but labeling efficiency was modest with a specific activity of 3 MBq/ $\mu\text{g}$ .  $^{99m}\text{Tc}$ -HYNIC-IL-8 accumulated rapidly in the abscess up to  $0.33 \pm 0.06$  percentage injected dose per gram (%ID/g) at 8 h after injection (vs.  $0.025 \pm 0.003$  %ID/g for  $^{99m}\text{Tc}$ -HYNIC-lysozyme). Total uptake in the abscess was  $4.9 \pm 0.7$  %ID (vs.  $0.44 \pm 0.05$  %ID for  $^{99m}\text{Tc}$ -HYNIC-lysozyme). Abscess-to-contralateral muscle ratios increased up to  $127 \pm 23$  (compared with  $6.7 \pm 1.1$  for  $^{99m}\text{Tc}$ -HYNIC-lysozyme) and abscess-to-blood ratios increased to  $11.9 \pm 2.2$  ( $0.24 \pm 0.03$  for  $^{99m}\text{Tc}$ -HYNIC-lysozyme). The radiolabel was excreted renally, with a retention in the kidneys of 28 %ID. Gamma camera imaging rapidly visualized the abscess from 1 h after injection onward, with abscess-to-background ratios improving with time up to 22 at 8 h after injection (vs. 2.7 for  $^{99m}\text{Tc}$ -HYNIC-lysozyme), as determined by quantitative analysis of the images. Most important, only a transient (30 min) moderate drop of leukocyte counts and no leukocytosis were observed after injection of an imaging dose of  $^{99m}\text{Tc}$ -HYNIC-IL-8. **Conclusion:** IL-8 can be labeled with  $^{99m}\text{Tc}$  using HYNIC as a chelator. By this method the leukocyte receptor-binding capacity is preserved. The preparation allows rapid visualization of infection in a rabbit model with high target-to-background ratios. The mild transient drop of leukocyte counts and the absence of leukocytosis suggest that  $^{99m}\text{Tc}$ -HYNIC-IL-8 may be used as an imaging agent with only mild and transient side effects.

**Key Words:** interleukin-8; infection; scintigraphic imaging; biodistribution;  $^{99m}\text{Tc}$

**J Nucl Med 2001; 42:117–123**

A wide range of radiopharmaceuticals has been proposed to visualize infection and inflammation scintigraphically. Use of autologous leukocytes, labeled with  $^{111}\text{In}$  or  $^{99m}\text{Tc}$ , is still considered the gold standard, nuclear medicine technique to image infection and inflammation. With regard to diagnostic accuracy, there is no need for a better imaging agent than labeled autologous leukocytes. However, the labeling procedure is time consuming and complex and could be hazardous. Therefore, there is a need for a radiopharmaceutical with at least similar clinical performance that can be prepared rapidly and easily. In the search for new agents to image infection and inflammation, the development of new radiopharmaceuticals has gradually shifted during the past decades: from large proteins with aspecific uptake mechanisms (e.g., IgG (*I-3*)) through receptor-specific proteins of large size (e.g., antigranulocyte (*4,5*) and antiE-selectin antibodies (*6*)) and moderate size (antibody fragments (*7*)) to small receptor-binding proteins and peptides (e.g., cytokines).

Labeled cytokines such as interleukin-1 (IL-1), interleukin-2 (IL-2), and interleukin-8 (IL-8) are a promising class of protein radiopharmaceuticals of small molecular weight (<20 kDa). Cytokines act through an interaction with specific cell-surface receptors expressed on known cell populations. Binding affinities are usually high (nanomolar range).

IL-1 binds receptors as expressed mainly on granulocytes, monocytes, and lymphocytes with high affinity. Studies in mice with focal *Staphylococcus aureus* infections showed specific uptake of radioiodinated IL-1 at the site of infection (infection-to-background ratios > 40 at 48 h after injection) (*8*). Unfortunately, the biologic effects (e.g., hypotension and headache) of IL-1, even at very low doses (10 ng/kg), precluded clinical application of radiolabeled IL-1.

Chronic inflammation is characterized by infiltration of the target tissue by lymphocytes. It was successfully targeted with radiolabeled IL-2 through specific binding to IL-2 receptors expressed on activated T lymphocytes. A method was developed that allowed the preparation of a  $^{99m}\text{Tc}$ -IL-2 preparation with a high specific activity (*9*). Studies in patients with insulin-dependent diabetes, Hashimoto's thyroiditis, Graves' disease, Crohn's disease, or celiac disease showed localization of  $^{123}\text{I}$ - or  $^{99m}\text{Tc}$ -IL-2 at the site of lymphocytic infiltration (*10*).

Received Feb. 16, 2000; revision accepted Jul. 28, 2000.

For correspondence or reprints contact: Huub J.J.M. Rennen, MSc, Department of Nuclear Medicine, University Medical Center Nijmegen, P.O. Box 9101, 6500 HB Nijmegen, The Netherlands.

IL-8 is a member of the CXC subfamily of the chemokines, or chemotactic cytokines, in which the first two cysteine residues are separated by one amino acid residue. IL-8 binds the CXC type I (IL-8 type A) and CXC type II (IL-8 type B) receptors expressed on neutrophils and monocytes with high affinity (0.3–4 nmol/L) (11,12). Hay et al. (13) studied the in vivo behavior of radioiodinated IL-8 in a rat model with carrageenan-induced sterile inflammation. The uptake peaked at 1–3 h after injection and declined thereafter. Target-to-background ratios did not exceed 2.5. These investigators showed that an  $^{125}\text{I}$ -IL-8 could visualize inflammatory foci in a pilot study of eight patients (14). We investigated the behavior and kinetics of radioiodinated IL-8 in various models of infection and sterile inflammation in rabbits (15,16). We found that IL-8 labeled according to the Bolton-Hunter (BH) method showed superior imaging characteristics. In rabbits with focal *Escherichia coli* infection, accumulation of  $^{125}\text{I}$ -IL-8 in the abscess was rapid and high ( $0.8 \pm 0.1$  percentage injected dose [%ID] 8 h after injection). Abscess-to-contralateral muscle ratios were  $>100$  in this model within 8 h after injection. The specific activity of this IL-8 preparation was relatively low; the imaging dose of  $^{125}\text{I}$ -IL-8 (25  $\mu\text{g}/\text{kg}$ ) caused a transient drop of peripheral leukocyte counts to 45%, which was followed by leukocytosis (170% of preinjection level) over a period of several hours.

For clinical imaging,  $^{125}\text{I}$  is not a very suitable radionuclide: It is expensive and the BH labeling method is rather laborious. For clinical application, a simple and rapid labeling procedure of IL-8, using the radionuclide  $^{99\text{m}}\text{Tc}$ , would be preferable. In this study we investigated the potential of  $^{99\text{m}}\text{Tc}$ -labeled IL-8 to image infections in a rabbit model. We aimed to develop a labeling technique that would result in a radiopharmaceutical with a high specific activity to decrease the IL-8 dose, thus reducing biologic activity. At the same time, the leukocyte receptor-binding capacity ought to be conserved. To accomplish this we used the bifunctional chelator hydrazinonicotinamide (HYNIC).  $^{99\text{m}}\text{Tc}$ -labeled lysozyme (14.3 kDa), with no specific receptor interaction, was used as a size-matched control in this study.

## MATERIALS AND METHODS

### Preparation of HYNIC Conjugates with IL-8

Human recombinant IL-8 was kindly provided by Dr. Ivan Lindley (Novartis, Vienna, Austria). Lysozyme was purchased from Sigma (St. Louis, MO). IL-8 was conjugated to HYNIC essentially as described by Abrams et al. (17). Briefly, 1.5  $\mu\text{L}$  1 mol/L  $\text{NaHCO}_3$ , pH 8.2, was added to 15  $\mu\text{L}$  IL-8 (5.7 mg/mL) in a 1.5-mL vial. Subsequently, succinimidyl-HYNIC (S-HYNIC) in 5  $\mu\text{L}$  dry dimethyl sulfoxide was added dropwise to the mixture. A series of conjugates was prepared using different molar conjugation ratios of IL-8:S-HYNIC (1:1–1:10) and different reaction times (3–60 min). After incubation at room temperature, the reaction was stopped by adding an excess of 1.0 mol/L glycine. Subsequently, precooled phosphate-buffered saline (PBS) was added to a total volume of 170  $\mu\text{L}$ . To remove excess unbound

S-HYNIC, the mixture was extensively dialyzed against PBS (0.1–0.5 mL dialysis cell, 3.5 molecular weight cutoff; Pierce, Rockford, IL). Dialyzed samples of  $\sim 7$   $\mu\text{g}$  IL-8-HYNIC were stored at  $-20^\circ\text{C}$ . Preparation of the lysozyme-HYNIC conjugate was similar; a 3-fold molar excess of S-HYNIC was used and the reaction was stopped after 3, 10, or 30 min.

### $^{99\text{m}}\text{Tc}$ Labeling of HYNIC-Conjugated IL-8

Tricine- $\text{SnSO}_4$  kits (0.2 mL) were prepared containing 20 mg *N*-[tris(hydroxymethyl)methyl]glycine (tricine; Fluka, Buchs, Switzerland) and 0.01 mg  $\text{SnSO}_4$  (Merck, Darmstadt, Germany) in 0.2 mL PBS, pH 7.0. To prevent precipitation of  $\text{Sn}^{2+}$ ,  $\text{SnSO}_4$  dissolved in 2 mol/L HCl was added to a solution of tricine in PBS and the pH was subsequently adjusted to 7.0 with 1.0 mol/L NaOH.

For receptor-binding assays, the HYNIC-conjugated IL-8 preparations with different molar conjugation ratios and different conjugation reaction times were labeled and tested. For animal studies, the HYNIC-IL-8 preparation that showed the best leukocyte receptor-binding capacity was selected for labeling and intravenous administration. As the control, an HYNIC-lysozyme preparation with the same reaction conditions was chosen. For receptor-binding assays, a 0.2-mL tricine- $\text{SnSO}_4$  kit and 0.1–0.3 mL 20–30 MBq  $^{99\text{m}}\text{TcO}_4^-$  in saline were added to 5  $\mu\text{g}$  thawed HYNIC-IL-8 and incubated at room temperature for 30 min. For animal studies, a 0.2-mL tricine- $\text{SnSO}_4$  kit and 0.5 mL 500 MBq  $^{99\text{m}}\text{TcO}_4^-$  in saline were added to 20  $\mu\text{g}$  thawed HYNIC-IL-8 or HYNIC-lysozyme and incubated at room temperature for 30 min. The radiochemical purity was determined by instant thin-layer chromatography (ITLC) on ITLC-SG strips (Gelman Laboratories, Ann Arbor, MI) with 0.1 mol/L citrate, pH 6.0, as the mobile phase.

After the labeling reaction, the reaction mixture was applied to a Sephadex G-25 column (PD-10; Pharmacia, Uppsala, Sweden) and eluted with 0.5% bovine serum albumin in PBS to purify the radiolabeled IL-8 or lysozyme conjugate.

### Receptor-Binding Assay

Human neutrophils were isolated from heparinized whole blood obtained from healthy donors. Receptor-binding assays were performed essentially as described (16) using  $^{99\text{m}}\text{Tc}$ -labeled IL-8 instead of radioiodinated IL-8.

### Animal Studies

Animal studies were performed essentially as described (16). The experiments were performed in accordance with the guidelines of the local animal welfare committee. Abscesses were induced in the left thigh muscle of 10 female New Zealand white rabbits (2.4–2.7 kg) with  $4 \times 10^{10}$  colony-forming units of *E. coli* in 0.5 mL. During the procedure, the rabbits were sedated with a subcutaneous injection of a 0.6-mL mixture of fentanyl (0.315 mg/mL) and fluanisone (10 mg/mL) (Hypnorm; Janssen Pharmaceutical, Buckinghamshire, UK). After 24 h, when swelling of the muscle was apparent, six rabbits were injected with 7 MBq  $^{99\text{m}}\text{Tc}$ -HYNIC-IL-8 (protein dose, 2.5  $\mu\text{g}$ ) in the ear vein. Three of them were used for gamma camera imaging (0, 1, 2, 4, and 8 h after injection), whereas the other three were used to determine the pharmacokinetics and to monitor white blood cell (WBC) counts. A control group of five rabbits was injected with 18 MBq  $^{99\text{m}}\text{Tc}$ -HYNIC-lysozyme (protein dose, 2.5  $\mu\text{g}$ ). Two of these animals were imaged with a gamma camera (0, 1, 2, 4, and 8 h after injection).

For imaging, rabbits were immobilized, placed prone on the gamma camera, and injected with either  $^{99m}\text{Tc}$ -HYNIC-IL-8 or  $^{99m}\text{Tc}$ -HYNIC-lysozyme in the lateral ear vein. Images were recorded at 1 min and at 1, 2, 4, and 8 h after injection with a single-head gamma camera (Orbiter; Siemens Medical Systems, Hoffman Estates, IL) equipped with a parallel-hole, low-energy, all-purpose collimator. Images (100,000–200,000 counts per image) were obtained and digitally stored in a  $256 \times 256$  matrix.

The scintigraphic results were analyzed quantitatively by drawing regions of interest over the abscess and the uninfected contralateral thigh muscle (background). Abscess-to-background ratios were calculated.

The pharmacokinetics and WBC counts were determined in a group of three rabbits injected with 7 MBq ( $2.5 \mu\text{g}$ )  $^{99m}\text{Tc}$ -HYNIC-IL-8. Blood samples were collected at  $-1, 1, 3, 5, 10, 30, 60, 120, 240,$  and 480 min after injection. Blood samples were weighed, their activity was measured, and their uptake was expressed as %ID/g tissue and as %ID in the blood pool on the basis of an estimated total blood volume of 6% of the total body weight of the rabbit (18). WBC counts were measured in the same blood samples and expressed as percentage of the preinjection value.

After completion of the final imaging and blood sampling (8 h after injection), the rabbits were killed with a lethal dose of sodium phenobarbital. Samples of blood, infected thigh muscle, uninfected contralateral thigh muscle, lung, spleen, liver, kidneys, and intestines were collected. The dissected tissues were weighed and counted in a gamma counter. Injection standards were counted simultaneously to correct for radioactive decay. The measured activity in samples was expressed as %ID/g. Additionally, total uptake of the radiopharmaceutical (%ID) was measured for kidneys and abscesses. Abscess-to-contralateral muscle ratios and abscess-to-blood ratios were calculated.

### Statistical Analysis

All mean values are given as %ID/g or ratios  $\pm 1$  SEM. The data were analyzed statistically using the one-way ANOVA.

## RESULTS

### Radiolabeling and Characterization of $^{99m}\text{Tc}$ -HYNIC-IL-8

The labeling efficiencies (%) and receptor-binding fractions (RBFs [%]) of various  $^{99m}\text{Tc}$ -HYNIC-IL-8 and  $^{99m}\text{Tc}$ -HYNIC-lysozyme preparations are shown in Table 1. An inverse relationship was found between labeling efficiency and leukocyte RBF. For animal studies the most mildly modified HYNIC-IL-8 preparation with the highest receptor-binding capacity was chosen (i.e., the preparation with a molar conjugation protein:S-HYNIC of 1:3 and a conjugation reaction time of 3 min). The conventional binding plot for this preparation is presented in Figure 1. As the control, the HYNIC-lysozyme preparation with the same molar conjugation ratio (1:3) and conjugation time (3 min) was chosen. The specific activity was  $2.8 \text{ MBq}/\mu\text{g}$  for the  $^{99m}\text{Tc}$ -HYNIC-IL-8 preparation and  $7.2 \text{ MBq}/\mu\text{g}$  for the  $^{99m}\text{Tc}$ -HYNIC-lysozyme preparation. The radiochemical purity of all radiopharmaceuticals was  $>95\%$  after gel filtration as determined by ITLC. In other experiments we used a more rigorously conjugated IL-8 preparation (protein:S-HYNIC, molar conjugation ratio 1:10; conjugation reaction time, 60 min.) (19). This preparation showed a

**TABLE 1**  
Labeling Efficiencies and RBFs of Various  $^{99m}\text{Tc}$ -HYNIC-IL-8 and  $^{99m}\text{Tc}$ -HYNIC-Lysozyme Preparations

Protein	Protein:S-HYNIC*	Reaction time (min)	Labeling efficiency† (%)	RBF (%)
IL-8	1:1	3	15	65
IL-8	1:1	60	87	31
IL-8	1:2	60	94	24
IL-8	1:3	3	20	65
IL-8	1:3	10	71	37
IL-8	1:3	30	83	30
IL-8	1:3	60	95	21
IL-8	1:10	60	97	16
Lysozyme	1:3	3	69	ND
Lysozyme	1:3	10	90	ND
Lysozyme	1:3	30	95	ND

\*Molar conjugation ratio.

†For determination of labeling efficiencies,  $5 \mu\text{g}$  HYNIC-conjugated protein were used with 20–30 MBq  $^{99m}\text{Tc}$ .

ND = not determined.

labeling efficiency of 97% with specific activities as high as  $75 \text{ MBq}/\mu\text{g}$ . However, the leukocyte receptor-binding capacity was greatly reduced (RBF, 16%), indicating that the conjugation conditions were too aggressive and modifications occurred in regions of the protein that are critical for receptor binding.

### $^{99m}\text{Tc}$ -HYNIC-IL-8 in Rabbits with *E. coli* Infection

Immediately after injection of  $^{99m}\text{Tc}$ -HYNIC-IL-8 ( $1 \mu\text{g}/\text{kg}$  body weight), a transient reduction of peripheral leukocyte levels to 54% was observed (Fig. 2). The WBC count returned to base levels within 30 min. No subsequent leukocytosis was observed. The blood clearance pattern fitted a two-phase model with a half-life ( $t_{1/2\alpha}$ ) of 4.2 min during the distribution phase and a half-life ( $t_{1/2\beta}$ ) of 5.1 h during the elimination phase (Fig. 3).

The abscesses were clearly delineated on the images recorded from 1 h onward (Fig. 4).  $^{99m}\text{Tc}$ -HYNIC-IL-8 rapidly accumulated at the site of infection. Quantitative analysis of the images indicated that the abscess-to-background ratios improved with time up to  $21.8 \pm 1.0$  at 8 h after injection (Fig. 5). High kidney uptake was observed immediately after injection; kidney uptake remained high during the 8 h after injection. In addition, activity was found in bladder, liver, and lungs. The control agent  $^{99m}\text{Tc}$ -HYNIC-lysozyme showed a similar kidney uptake pattern but failed to accumulate significantly at the site of infection. Abscess-to-background ratios did not exceed 2.7 (Fig. 5).

Tissue biodistribution of the radiolabel determined at 8 h after injection is summarized in Table 2. Except for the kidneys and the spleen, the highest uptake of  $^{99m}\text{Tc}$ -HYNIC-IL-8 was found in the abscess:  $0.33 \pm 0.06 \text{ %ID/g}$  versus  $0.025 \pm 0.003 \text{ %ID/g}$  for  $^{99m}\text{Tc}$ -HYNIC-lysozyme ( $P = 0.0001$ ). Total uptake in the infected tissue was  $4.9 \pm 0.7$

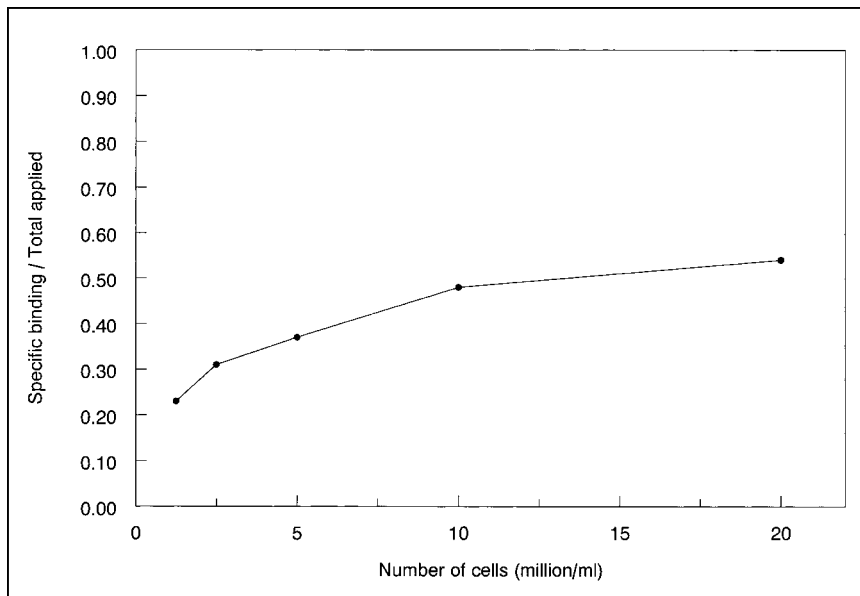


**FIGURE 1.** Conventional binding plot of  $^{99m}\text{Tc}$ -HYNIC-IL-8 as determined on isolated human granulocytes. Specific binding over total applied radioactivity is plotted as function of increasing cell concentration.

%ID versus  $0.44 \pm 0.05$  %ID for  $^{99m}\text{Tc}$ -HYNIC-lysozyme ( $P = 0.0001$ ), indicating preferential retention of IL-8 in infected tissue. Abscess-to-contralateral muscle ratios reached a value as high as  $127 \pm 23$  at 8 h after injection versus  $6.7 \pm 1.1$  for  $^{99m}\text{Tc}$ -HYNIC-lysozyme ( $P < 0.001$ ). The abscess-to-blood ratio was  $11.9 \pm 2.2$  at 8 h after injection compared with  $0.24 \pm 0.03$  for  $^{99m}\text{Tc}$ -HYNIC-lysozyme ( $P = 0.0001$ ). Kidney retention was high: At 8 h after injection,  $28 \pm 1$  %ID was found in the kidneys ( $35 \pm 1$  %ID for  $^{99m}\text{Tc}$ -HYNIC-lysozyme).

## DISCUSSION

On the basis of results with radioiodinated IL-8 obtained previously in our laboratory, we explored the potential of

$^{99m}\text{Tc}$ -labeled IL-8 to image infection and inflammation in rabbits with *E. coli* infection. This study showed that IL-8 can be labeled with  $^{99m}\text{Tc}$ , using HYNIC as a chelator, with preservation of its leukocyte receptor-binding capacity. The preparation allows rapid visualization of infection within a few hours after injection and high target-to-background ratios. The mild transient drop of leukocyte counts and the absence of leukocytosis suggest that  $^{99m}\text{Tc}$ -HYNIC-IL-8 may be applied as a clinically useful imaging agent.

The labeling efficiency and leukocyte receptor-binding capacity of various  $^{99m}\text{Tc}$ -HYNIC-IL-8 preparations was tested. Mildly modified  $^{99m}\text{Tc}$ -HYNIC-IL-8 preparations showed good receptor binding but modest  $^{99m}\text{Tc}$  binding, with a relatively low specific activity of nearly  $3 \text{ MBq}/\mu\text{g}$ .

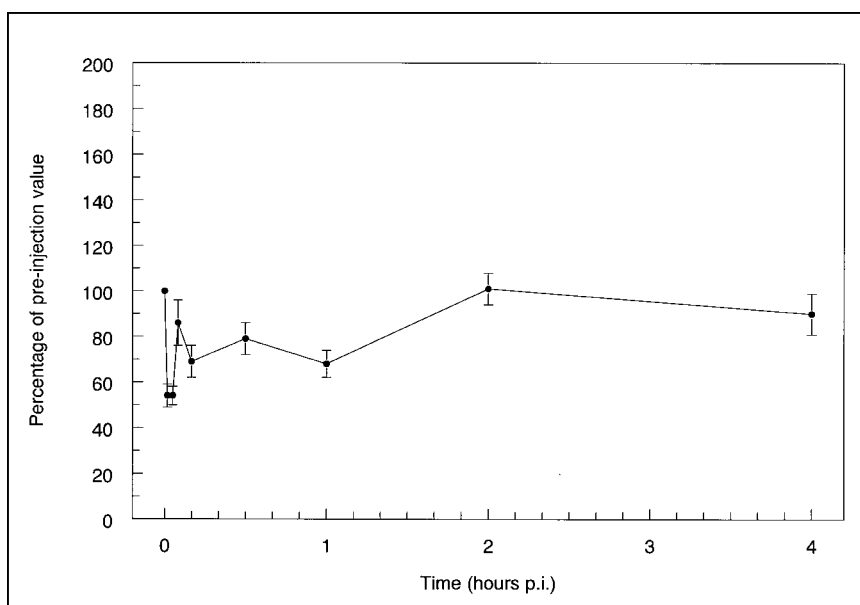


**FIGURE 2.** WBC counts in blood of *E. coli*-infected New Zealand white rabbits after intravenous injection of  $2.5 \mu\text{g}$   $^{99m}\text{Tc}$ -HYNIC-IL-8, expressed as percentage of preinjection value. Error bars indicate SEM. p.i. = after injection.

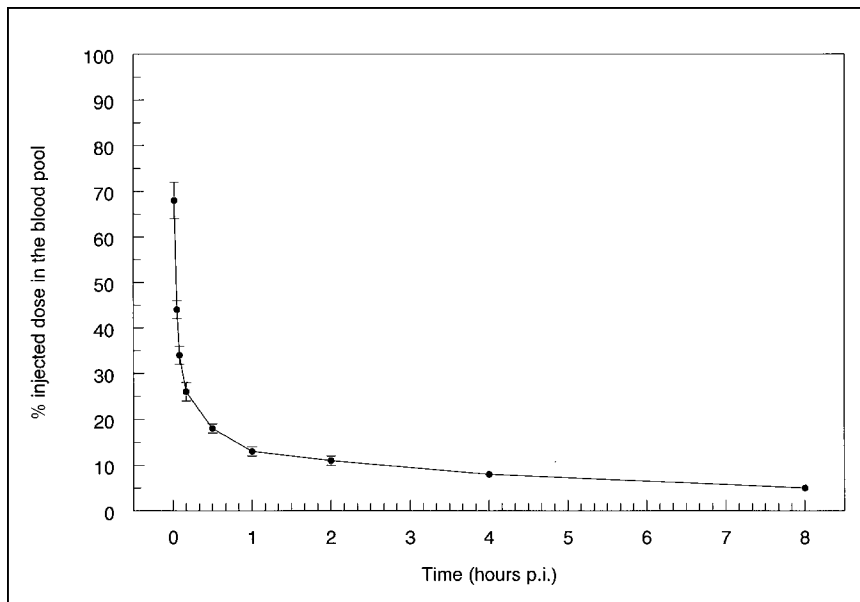


**FIGURE 3.** Blood clearance of <sup>99m</sup>Tc-HYNIC-IL-8 determined in rabbits with *E. coli* infection. Data are expressed as %ID in blood pool. Error bars indicate SEM. p.i. = after injection.

On the other hand, more rigorous conjugation of IL-8 with S-HYNIC resulted in <sup>99m</sup>Tc-HYNIC-IL-8 preparations with high specific activities (as high as 75 MBq/ $\mu$ g), but with a severe loss of receptor-binding capacity. The best infection imaging characteristics were obtained with the mildly modified <sup>99m</sup>Tc-HYNIC-IL-8 preparation reported in this study. This was shown, for instance, by an abscess-to-muscle ratio of 127 at 8 h after injection compared with 36 for the more rigorously conjugated IL-8 preparation used formerly (19).

The observation that abscess uptake of <sup>99m</sup>Tc-HYNIC-IL-8 was >10 times higher than the uptake of <sup>99m</sup>Tc-HYNIC-lysozyme suggested that abscess uptake was a result of the interaction of IL-8 with its receptors in the infectious foci. Specific uptake was shown also by an abscess-to-muscle ratio of 127 compared with 6.7 for the control peptide. Uptake in the kidneys was high for both peptides, which is a common phenomenon for radiolabeled peptides (20–24). The mechanism of renal uptake and re-

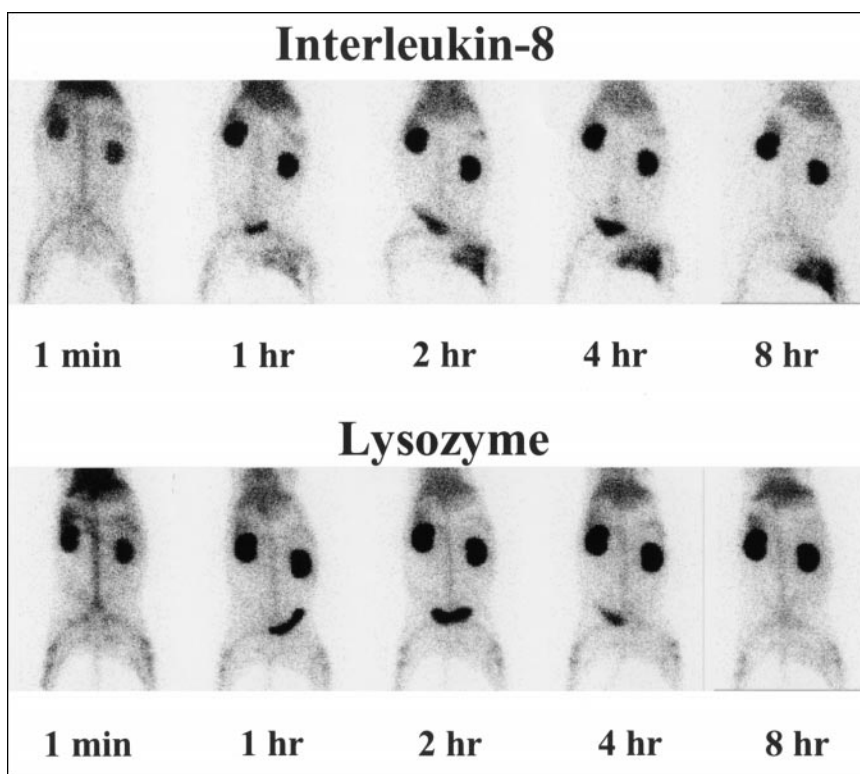
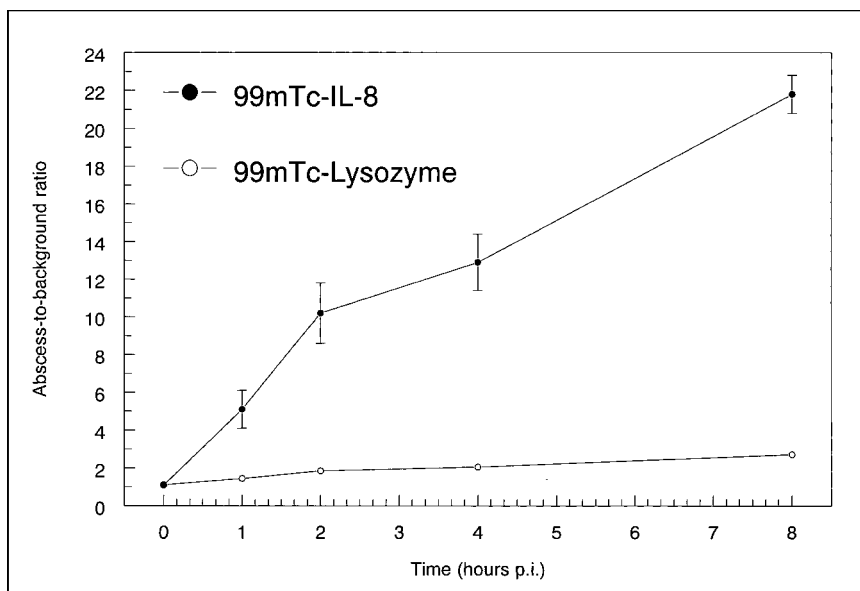


**FIGURE 4.** Images of rabbits with *E. coli* abscess in left thigh muscle at 1 min and at 1, 2, 4, and 8 h after injection of <sup>99m</sup>Tc-HYNIC-IL-8 (top) or <sup>99m</sup>Tc-HYNIC-lysozyme (bottom). All photographs were produced with same image contrast.

**FIGURE 5.** Abscess-to-background ratios as determined by quantitative analysis of images of rabbits with *E. coli* infection injected with  $^{99m}\text{Tc}$ -HYNIC-IL-8 (●) or  $^{99m}\text{Tc}$ -HYNIC-lysozyme (○). Error bars indicate SEM. p.i. = after injection.



tention of proteins is believed to involve glomerular filtration and subsequent reabsorption and catabolism in the proximal tubular cells (25,26). This process is dependent on molecular weight and charge of the proteins. Proteins exceeding a size of ~60 kDa are too large to pass the glomerular basement membrane and thus are not retained in the kidneys. Cationic proteins, in contrast to anionic proteins, are preferably retained in the kidneys. Several investigators have reduced renal uptake by infusing basic amino acids

such as lysine and arginine (26). Other strategies involve chemical modification of the protein. A substantial reduction of renal uptake has been achieved by glycolation of free amino groups (lysine side chains) (27,28).

IL-8 has been investigated for scintigraphic detection of infection and inflammation by Hay et al. (13) and by Van der Laken et al. (15,16) in our laboratory. In these studies IL-8 was radioiodinated using the chloramine-T, the Iodogen (Pierce), or the BH method. The BH method was found to be superior. With iodinated IL-8 prepared using the BH method ( $^{123}\text{I}$ -BH-IL-8), abscess-to-muscle and abscess-to-blood ratios of 115 and 12, respectively (8 h after injection), were obtained in a rabbit model, similar to the ratios obtained in this study. With both preparations, abscesses were visualized as early as 1 h after injection. Uptake of activity in the kidneys was high with both preparations, although it was less pronounced for  $^{123}\text{I}$ -BH-IL-8. The difference is caused by clearance of the radioiodinated label from the tubular cells after degradation in the lysosomes, whereas radiometal chelates remain trapped within lysosomes (21,26–28). Labeling IL-8 with  $^{99m}\text{Tc}$  using HYNIC offers great advantages over the BH iodination method. First, compared with  $^{123}\text{I}$ -BH-IL-8, the preparation of  $^{99m}\text{Tc}$ -HYNIC-IL-8 is easy, fast, and suitable for instant kit formulations for routine use. Second, a formulation with  $^{99m}\text{Tc}$  is inexpensive and always available compared with  $^{123}\text{I}$ . Most important, a preparation with much higher specific activity can be obtained. In this way the amount of biologically active material injected is reduced 25-fold: 1  $\mu\text{g}/\text{kg}$   $^{99m}\text{Tc}$ -HYNIC-IL-8 versus 25  $\mu\text{g}/\text{kg}$   $^{123}\text{I}$ -BH-IL-8. Using a dose of 25  $\mu\text{g}/\text{kg}$ , IL-8 induced transient leukopenia followed by leukocytosis over a period of several hours (15), whereas at a dose level of 1  $\mu\text{g}/\text{kg}$  only a mild transient drop of leukocyte counts without subsequent leukocytosis was observed. This suggests that  $^{99m}\text{Tc}$ -HYNIC-IL-8 can be

**TABLE 2**  
Biodistribution of  $^{99m}\text{Tc}$ -HYNIC-IL-8 and  $^{99m}\text{Tc}$ -HYNIC-Lysozyme in Rabbits with *E. coli* Infections at Eight Hours After Injection

Organ	%ID/g	
	$^{99m}\text{Tc}$ -HYNIC-IL-8 (n = 6)	$^{99m}\text{Tc}$ -HYNIC-lysozyme (n = 5)
Blood	0.028 ± 0.001	0.105 ± 0.006
Abscess	0.33 ± 0.06	0.025 ± 0.003
Muscle	0.0026 ± 0.0001	0.0041 ± 0.0008
Lung	0.19 ± 0.04	0.077 ± 0.011
Spleen	0.64 ± 0.06	0.119 ± 0.005
Kidney	1.47 ± 0.06	1.77 ± 0.06
Liver	0.14 ± 0.01	0.124 ± 0.006
Intestine	0.025 ± 0.002	0.028 ± 0.001
<b>Ratio</b>		
Abscess-to-muscle	127 ± 23	6.7 ± 1.1
Abscess-to-blood	11.9 ± 2.2	0.24 ± 0.03
<b>Total uptake</b>		
Infected tissue (%ID)	4.9 ± 0.7	0.44 ± 0.05
Kidneys (%ID)	28 ± 1	35 ± 1

Values are expressed as mean ± SEM.

used as an imaging agent potentially without clinically significant side effects.

In addition to IL-8, several small  $^{99m}\text{Tc}$ -labeled peptides capable of binding to leukocytes *in vivo* have been developed and tested for their imaging qualities.  $^{99m}\text{Tc}$ -labeled *N*-formyl-methionyl-leucyl-phenylalanyl-lysine (fMLFK) (29) and platelet factor 4–derived peptide P483H (30) are effective infection-seeking agents. However, in the same animal model, abscess-to-muscle ratios obtained with these agents were only a quarter of those obtained with IL-8. In addition, fMLFK showed relatively high activity in bowel and liver, resulting in high background activity and making this imaging agent less suitable for detection of infections in the abdomen.

Future experiments with  $^{99m}\text{Tc}$ -labeled IL-8 will focus on improvement of the labeling efficiency without compromising the receptor-binding activity and infection-localizing capacity of the agent. Site-specific attachment of a bifunctional chelating group in a region of IL-8 not critical for receptor binding will be the proper solution.

## CONCLUSION

This study showed that  $^{99m}\text{Tc}$ -labeled IL-8 has excellent characteristics as an infection imaging agent: It rapidly accumulated in infectious foci, while it rapidly cleared from non-target tissues. The technetium chemistry allowed labeling of IL-8 with preservation of its leukocyte receptor-binding capacity. The mild transient drop of leukocyte counts without subsequent leukocytosis suggests that  $^{99m}\text{Tc}$ -HYNIC-IL-8 may be a clinically useful imaging agent without significant side effects. These results warrant further development of an IL-8–based radiopharmaceutical for imaging of infection.

## ACKNOWLEDGMENTS

The authors thank Gerrie Grutters (Central Animal Laboratory, University of Nijmegen) and Emile Koenders (Department of Nuclear Medicine, University Medical Center Nijmegen) for their excellent technical assistance.

## REFERENCES

- Oyen WJG, Claessens RAMJ, van der Meer JWM, Corstens FHM. Biodistribution and kinetics of radiolabelled proteins in rats with focal infection. *J Nucl Med*. 1992;33:388–394.
- Buscombe JR, Oyen WJG, Grant A, et al. Indium-111-labeled human polyclonal immunoglobulin: identifying focal infection in patients positive for human immunodeficiency virus (HIV). *J Nucl Med*. 1993;34:1621–1625.
- Babich JW, Graham W, Barrow SA, Fischman AJ. Comparison of the infection imaging properties of a  $^{99m}\text{Tc}$  labeled chemotactic peptide with  $^{111}\text{In}$  IgG. *Nucl Med Biol*. 1995;22:643–648.
- Becker W, Goldenberg DM, Wolf F. The use of monoclonal antibodies and antibody fragments in the imaging of infectious lesions. *Semin Nucl Med*. 1994;24:142–153.
- Thakur ML, Marcus CS, Henneman P, et al. Imaging inflammatory diseases with neutrophil-specific technetium-99m-labeled monoclonal antibody anti-SSEA-1. *J Nucl Med*. 1996;37:1789–1795.
- Keelan E, Chapman P, Binns R, Peters A, Haskard D. Imaging vascular endothelial activation: an approach using radiolabeled monoclonal antibodies against the endothelial cell adhesion molecule E-selectin. *J Nucl Med*. 1994;35:276–281.
- Becker W, Palestro CJ, Winship J, et al. Rapid imaging of infections with a monoclonal antibody fragment (Leukoscan). *Clin Orthop*. 1996;329:263–272.
- Van der Laken CJ, Boerman OC, Oyen WJG, et al. Specific targeting of infectious foci with radioiodinated human recombinant interleukin-1 in an experimental model. *Eur J Nucl Med*. 1995;22:1249–1255.
- Chianelli M, Signore A, Fritzsche AR, Mather SJ. The development of technetium-99m-labelled interleukin-2: a new radiopharmaceutical for the *in vivo* detection of mononuclear cell infiltrates in immune-mediated diseases. *Nucl Med Biol*. 1997;24:579–586.
- Signore A. Interleukin-2 scintigraphy: an overview [abstract]. *Nucl Med Commun*. 1999;20:938.
- Lee J, Horuk R, Rice GC, Bennett GL, Camerato T, Wood WI. Characterization of two high affinity human interleukin-8 receptors. *J Biol Chem*. 1992;267:16283–16287.
- Cerretti DP, Kozlosky CJ, VandenBos T, Nelson N, Gearing DP, Beckmann MP. Molecular characterization of receptors for human interleukin-8, GRO/melanoma growth-stimulatory activity and neutrophil activating peptide-2. *Mol Immunol*. 1993;30:359–367.
- Hay RV, Skinner RS, Newman OC, et al. Scintigraphy of acute inflammatory lesions in rats with radiolabelled recombinant human interleukin-8. *Nucl Med Commun*. 1997;18:367–378.
- Gross MD, Shapiro B, Skinner RS, Shreve P, Fig LM, Hay RV. Scintigraphy of osteomyelitis in man with human recombinant interleukin-8 [abstract]. *J Nucl Med*. 1996;37(suppl):25P.
- Van der Laken CJ, Boerman OC, Oyen WJ, Van de Ven MT, Ven der Meer JW, Corstens FH. The kinetics of radiolabelled interleukin-8 in infection and sterile inflammation. *Nucl Med Commun*. 1998;19:271–281.
- Van der Laken CJ, Boerman OC, Oyen WJ, Van de Ven MT, Van der Meer JW, Corstens FH. Radiolabeled interleukin-8: specific scintigraphic detection of infection within a few hours. *J Nucl Med*. 2000;41:463–469.
- Abrams MJ, Juweid M, tenKate CI, et al. Technetium-99m-human polyclonal IgG radiolabeled via the hydrazino nicotinamide derivative for imaging focal sites of infection in rats. *J Nucl Med*. 1990;31:2022–2028.
- Jain NC. Blood volume and water balance. In: Jain NC, ed. *Schalm's Veterinary Hematology*. 4th ed. Philadelphia, PA: Lea & Febiger; 1986:87–102.
- Rennen HJMM, Boerman OC, Oyen WJG, Van der Laken CJ, Corstens FHM. Specific and rapid scintigraphic detection of infection with Tc-99m-labeled interleukin-8 [abstract]. *Eur J Nucl Med*. 1999;26:1005.
- Maack T, Park CH, Camargo MJF. Renal filtration, transport, and metabolism of proteins. In: Seldin DW, Giebisch G, eds. *The Kidney: Physiology and Pathophysiology*. 2nd ed. New York, NY: Raven Press; 1992:3005–3038.
- Behr TM, Sharkey RM, Sgouros G, et al. Overcoming the nephrotoxicity of radiometal-labeled immunoconjugates: improved cancer therapy administered to a nude mouse model in relation to the internal radiation dosimetry. *Cancer*. 1997;80:2591–2610.
- Kobayashi H, Le N, Kim IS, et al. The pharmacokinetic characteristics of glycolated humanized anti-Tac Fabs are determined by their isoelectric points. *Cancer Res*. 1999;59:422–430.
- Kobayashi H, Kim IS, Drumm D, et al. Favorable effects of glycolate conjugation on the biodistribution of humanized antiTac Fab fragment. *J Nucl Med*. 1999;40:837–845.
- Kim IS, Yoo TM, Kobayashi H, et al. Chemical modification to reduce renal uptake of disulfide-bonded variable region fragment of anti-Tac monoclonal antibody labeled with  $^{99m}\text{Tc}$ . *Bioconjugate Chem*. 1999;10:447–453.
- Sumpio BE, Maack T. Kinetics, competition and selectivity of tubular absorption of proteins. *Am J Physiol*. 1982;243:F379–F392.
- Behr TM, Goldenberg DM, Becker W. Reducing the renal uptake of radiolabeled antibody fragments and peptides for diagnosis and therapy: present status, future prospects and limitations. *Eur J Nucl Med*. 1998;25:201–212.
- Naruki Y, Carrasquillo JA, Reynolds JC, et al. Differential cellular catabolism of  $^{111}\text{In}$ -90-Y and  $^{125}\text{I}$  radiolabeled T101 anti-CD5 monoclonal antibody. *Int J Radiat Appl Instr*. 1990;17:201–207.
- Sakahara H, Saga T, Endo K, et al. *In vivo* instability of reduction-mediated  $^{99m}\text{Tc}$ -labeled monoclonal antibody. *Nucl Med Biol*. 1993;20:617–623.
- Van der Laken CJ, Boerman OC, Oyen WJ, et al. Technetium-99m-labeled chemotactic peptides in acute infection and sterile inflammation. *J Nucl Med*. 1997;38:1310–1315.
- Moyer BR, Vallabhajosula S, Lister-James J, et al. Technetium-99m-WBC-specific imaging agent developed from platelet factor 4 to detect infection. *J Nucl Med*. 1996;37:673–679.



The Journal of  
NUCLEAR MEDICINE

## Specific and Rapid Scintigraphic Detection of Infection with $^{99m}\text{Tc}$ -Labeled Interleukin-8

Huub J.J.M. Rennen, Otto C. Boerman, Wim J.G. Oyen, Jos W.M. van der Meer and Frans H.M. Corstens

*J Nucl Med.* 2001;42:117-123.

---

This article and updated information are available at:  
<http://jnm.snmjournals.org/content/42/1/117>

---

Information about reproducing figures, tables, or other portions of this article can be found online at:  
<http://jnm.snmjournals.org/site/misc/permission.xhtml>

Information about subscriptions to JNM can be found at:  
<http://jnm.snmjournals.org/site/subscriptions/online.xhtml>

*The Journal of Nuclear Medicine* is published monthly.  
SNMMI | Society of Nuclear Medicine and Molecular Imaging  
1850 Samuel Morse Drive, Reston, VA 20190.  
(Print ISSN: 0161-5505, Online ISSN: 2159-662X)

© Copyright 2001 SNMMI; all rights reserved.